Electrical energy is generated by harvesting the induced charge in metal electrodes and by connecting the surface of the taro leaf, coated with the electrodes underneath, to the bridge rectifier and capacitor. This discussion was supported by a Scanning Electron Microscope analysis on the surface of taro leaves. The electrical energy was measured using a bridge rectifier at various water droplet rate in contact with leaf, and at various slope of the taro leaves. The results showed that the slope of the leaf surface contact area with water droplets and taro leaf increases the generation of electric voltage. The greater the tilt angle of the taro leaf surface causing more electrons to jump out of orbit. The surface of taro leaves made by a cluster of nanostalagmites with other nanostalagmites separated by nanoscale hollows that tend to repel water droplets. The results from the repulsion of nanostalagmites at a very small radius of the nanostalagmite structure were very high surface tension or surface energy. The electron jump is mainly generated due to the high surface tension energy of the nanostalagmite structure that when it comes into contact with ionized H^+ and OH^- in the water droplet, it produces hydrogen (H_2). H_2 is trapped in the nanohollows between the nanostalagmites. Due to the dense morphology of nanostalagmite, H_2 will tend to be pushed upwards to force the water droplet. As a result, the surface tension will be higher and the surface will be more superhydropobic thereby increasing the electrical voltage. The morphology and the tilt angle have an important role in generating electrical energy. Thus, it is necessary to do further research on superhidrophobic characteristics as a solution in the future to overcome the problem of electrical energy

Keywords: water droplet, nanohollow, nano-stalagmite, superhydrophobic surface, taro leaf, electrical energy

UDC 620
DOI: 10.15587/1729-4061.2020.214263

DEVELOPMENT OF ENERGY HARVESTING WITH WATER DROPLET CONTINUOUS FLOW OVER NANOHOLLOW AND NANOSTALAGMITE OF TARO LEAF SURFACE

Komang Metty Trisna Negara
Doctoral Student in Mechanical Engineering*
Study Program in Mechanical Engineering
Department of Mechanical Engineering
Samawa University
Great Sumbawa, West Nusa Tenggara, Indonesia
E-mail: mettytrisnan@gmail.com
Nurkholis Hamidi
Doctorate in Mechanical Engineering*
E-mail: hamidy@ub.ac.id
Denny Widhiyanuriyawan
Doctorate in Mechanical Engineering*
E-mail: Denny_w@ub.ac.id
I Nyoman Gede Wardana
Professor in Mechanical Engineering*
E-mail: wardana@ub.ac.id
*Department of Mechanical Engineering
Brawijaya University
Jl. Mayjend Haryono, 167, Malang, Indonesia, 65145

Received date 03.09.2020
Accepted date 15.10.2020
Published date 31.10.2020

1. Introduction

In the last decades, global warming and climate change have become the most important environmental issues due to rampant consumption of fossil fuels. Fossil fuels are a very limited resource, prices will continue to increase as reserves continue to decrease. Therefore, efforts to increase renewable and environmentally friendly energy sources have been devoted. As such, the use of environmentally friendly materials such as the use of materials from plants, insects and pseudo-superhydrophobic organisms is being widely studied at present [1].

Technologies that have been developed on a small scale to produce wasted energy have had tremendous results. Energy from water droplets is another attractive energy source for low power applications such as sensors and portable electronics. Recently it is reported that the surface of taro leaves can generate electrical energy when it comes into contact with a water droplet [2]. However, it is necessary to investigate the attainment of electrical energy in more depth if the water droplets are continuously contacted.

Therefore, studies that are devoted are on morphological characteristics of taro leaves is required. In this study, the characteristics were studied on the surface of taro leaves. The characteristics of taro leaves are generated by functional groups built in nanostalagmite structures separated by nanoscale hollows. Detail discussions are made on how the interaction between functional groups in the nanostalagmite structure separated by nanoscale hollows with water droplet could kick electrons out from their orbits to produce electrical energy. In addition, the other purpose of this study is as one of the solutions in the future to overcome the problem in harvesting energy.

2. Literature review and problem statement

In previous research, various micro energy harvesting technologies of producing electrical energy have been developed. Some of them use ambient acoustic noise harvested by an actuator using acoustically oscillating liquid droplets [3], sequential contact-electrification and electrostatic-induction processes [4]. Contact electrification, also called triboelectrification, is a well-known phenomenon that occurs when two materials come into contact, and has been shown in applications such as metal ion reduction [5–7], electrostatic charge plates [8, 9], sensor chemicals [10], and laser printing. This phenomenon has been used to collect energy from environmental sources, in the form of a triboelectric nanogenerator (TENG) [11–13]. Typically, TENG requires a relatively dry environment to produce a stable output [14, 15], because the triboelectrification surface will be reduced due to the presence of water. As such, energy sources related to water, such as ocean waves, waterfalls, and rainwater that have an abundant amount of energy and are inexhaustible, can be a good option as alternative energy. Water droplet energy such as raindrop is another attractive energy source for low power applications such as sensors and portable electronics [16]. Harvesters based on piezoelectric materials consisting of polyvinylidene difluoride (PVDF) and lead zirconate titanate (PZT) have shown the potential to convert the mechanical impact energy of water droplets into electricity [17, 18].

In this study, the ability of the superhydrophobic properties of taro leaves (colocasiaesculenta L) to generate electrical energy is described in more depth. When the droplets are dropped on a certain surface, a contact angle is formed, which is highly dependent on the hydrophobicity [19, 20]. The contact angle (θ) is created by the geometric intersection between the liquid-solid and gas-liquid surfaces (water droplets and leaf surfaces), creating a tangent towards the line of contact with the line crossing the water droplet base [21]. This will be easy to a reader to understand, if to add the figure with comments.

As shown in Fig. 1 based on the shape of the water droplets and the contact angle made, the surface is classified as hydrophilic when the contact angle is $\theta<30^\circ$, hydrophobic when the contact angle is $90^\circ<\theta<120^\circ$, overhydrophobic when the contact angle is $120<\theta<150^\circ$, and superhydrophobic when the contact angle is $\theta> 150^\circ$ [22–24]. In addition, the surface tension that occurs between water and the superhydrophobic surface of taro leaves was identified as having the ability to generate hydrogen gas [25].

Among the various types of energy harvesting technologies, energy harvesting by utilizing small water droplets based on the superhydropobic contact area is the most popular because of its simple structure. However, there were unresolved issues, this study only focuses on applied experimental research and hardly reveal any fundamental scientific information about the interaction between the morphological structures of the superhydrophobic surface and water droplets when continuously contacted. The impact of water droplets hitting a superhydropobic surface on a taro leaf creates a jump into an electric voltage. The envisioned energy harvesting system uses small water with continuous droplets to convert the impact energy into electrical energy. This new energy harvesting method is a simple, cheap and environmental friendly. Moreover, the uniqueness and role of superhydrophobic materials are difficult to understand at the application based research level. Thus, it is necessary to do further research on superhydrophobic characteristics as a solution in the future to overcome the problem of electrical energy.

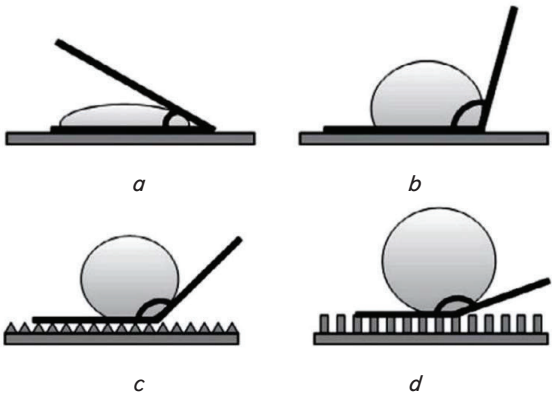

Fig. 1. Classification of surface with droplets forms a contact angle θ; *a* – Hydrophilic surface $\theta<30^\circ$; *b* – Hydrophobic surface $90^\circ<\theta<120^\circ$; *c* – Overhydrophobic surface $120^\circ<\theta<150^\circ$; *d* – Superhydrohobic surface $\theta<150^\circ$ (Source: [22])

3. The aim and objectives of the study

This research aims to produce new discoveries in the energy sector since the energy obtained is in the form of energy that is environmentally friendly and has no polluting effect.

To achieve this aim, the following objectives were set:

– to find out the mechanism for the generation of electrical energy using natural materials from plants, namely taro leaves (*Colocasia Esculenta L*) and tilt effect on the resulting voltage, in the electric energy harvesting model;

– to reveal the interaction between functional groups in the nanostalagmite and nanohollow structure to produce electrical energy.

4. Materials and methods of research

The research that was conducted was experimental research. The superhydrophobic surface was made using taro leaves which have a surface area of 1×3 cm^2 an aluminum foil electrode with a surface was attached to the underside of the taro leaves. Fig. 2 shows a series of all research installation units where the far right is aluminum foil and taro leaves are attached on top. Then they were connected to the bridge rectifier with a sensor cable. The rectifier bridge sensor cable was connected to the taro leaf and the other sensor cable was connected to the aluminum foil. This bridge rectifier write a number was connected to a capacitor write voltage and capacity as well as the type and moreover, this sign is used for chemical power sources (when one line shorter than other) change it as follows (as one from capacitors from series).

Bridge rectifier used one small round part, type (SMC-0024) 2W10. Maximum repetitive peak reverse voltage: 1000 V. Maximum RMS bridge input voltage: 700 V. Maximum DC blocking voltage: 1000 V. Maximum average forward rectified output current (at TA=25)

IF: 2 A. Maximum forward voltage per diode (at IF=1.0 A) VF: 1 V. Operating junction and storage temperature range: –55 to +150 °C. The use of this bridge rectifier is to replace the diode model that uses 4 diodes. There are 4 pins, 2 pins for AC input and 2 pins for DC output. One electrolyte capacitor with a capacity of 10 V 33 uF is connected parallel to a bridge rectifier, then to the measuring instrument of digital multimeter.

The location of the leaves and electrodes of the aluminum foil with a cable connected to the 2 pins for the AC input on the bridge rectifier is shown in Table 1.

Data collection began when water droplets were dropped vertically from the top of the leaves at a rate of 1 drop/s, 2 drops/s, 3 drops/s continuously and with variations in the slope of the fields 0°, 15°, 30°, and 45°. Electric voltage occurred when water droplets came into contact with the leaf surface which has a waxy coating. The existence of a bridge rectifier functions to deliver the AC current arises from the water droplets in contact with the taro leaves to become a DC current. Therefore, the diode circuit in the form of a bridge rectifier is used in this test as a current rectifier. Furthermore, on the right side of the bridge rectifier there is a capacitor with a capacity of 33 μF. The electrons generated from the water droplet in contact with the taro leaves will be stored in the capacitor for a certain time as long as there is no conduction at the ends of the capacitor's legs. The magnitude of the electron jump will be read as the voltage on a voltage detector in the form of a digital multimeter. This event was recorded by a digital multimeter connected to a laptop. The travel of water droplets across the entire 3 cm leaf area was observed using a high-speed camera. Voltage data collection was taken at various variations according to the variations in Table 2.

Each water droplet with a diameter of 4 mm has a mass of 0.04744 grams (weighed using a Toledo type XPE205 electronic mettle digital scale with a reading accuracy of 0.00001). The measuring instrument for the voltage is the Mastech MS8250C, China, Ltd series digital multimeter which has been calibrated using a 9000 series calibrator. The movement of water droplets on the taro leaves was observed using a high-speed, Keyence Co, Japan series macro zoom systems with a speed of 1000 frame/second and the VW-9000 high-speed microscope series, Keyence Co, USA. The surface morphology of taro leaves was tested using a FEI Inspect S-50 type SEM, Oregon USA, Ltd. (Scanning Electron Microscope). In observation, the voltage signal can only be generated and read by the multimeter if the taro leaves are in good condition, the location of the leaves is right on top of the aluminum, and the falling water droplets roll right along the plane path. When there is damage to the surface of the taro leaves, the voltage signal does not appear or cannot be read on the multimeter.

Variations in data collection were carried out to obtain the most appropriate combination to produce the greatest electrical energy. From the total variation, the process was repeated 3 times. Then the most optimal data was selected and presented in graphical form. These variations include: the quantity of water droplets falling on the leaf surface (3 drops/s, 2 drops/s, 1 drop/s) and the slope of the taro leaf area coated with aluminum foil 0°, 15°, 30°, 45°. Furthermore, the variations are presented in Table 2.

Table 1

The location of the taro leaves on the aluminum foil as an electrode at a slope of 0 °, 15 °, 30 °, 45 °

Location of the taro leaves on the aluminium foil	
Slope 0° 	Slope 15° 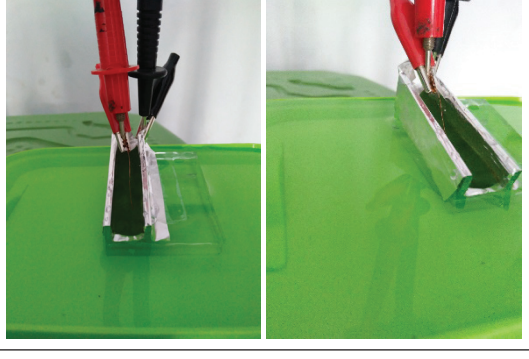
Slope 30° 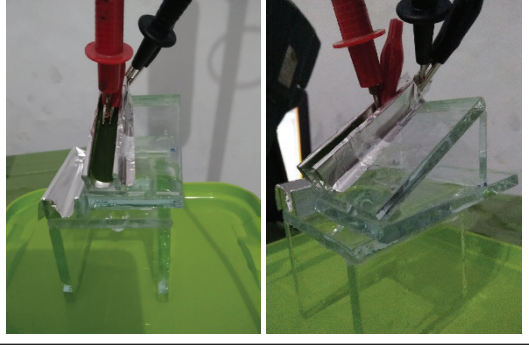	Slope 45° 

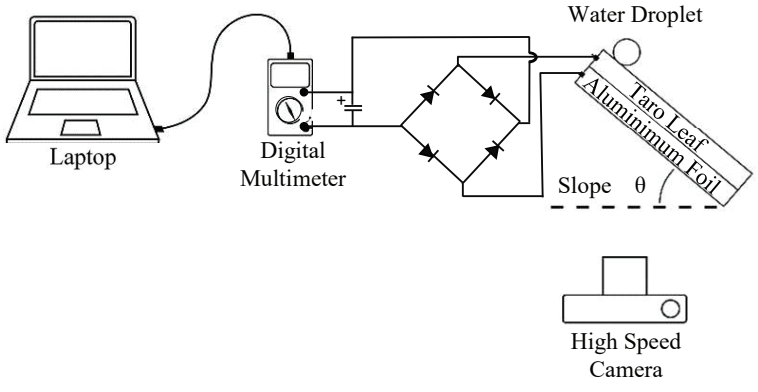

Fig. 2. Research installation on the superhydrophobic surface of taro leaves with continuous water droplets

Table 2

Variations in data collection

Variations in the slope of contact area and rate water droplet			
0°	15°	30°	45°
Droplet rate 1, drop/s	Droplet rate 1, drop/s	Droplet rate 1, drop/s	Droplet rate 1, drop/s
Droplet rate 2, drops/s	Droplet rate 2, drops/s	Droplet rate 2, drops/s	Droplet rate 2, drops/s
Droplet rate 3, drops/s	Droplet rate 3, drops/s	Droplet rate 3, drops/s	Droplet rate 3, drops/s

5. Results from development of energy harvesting with water droplet continuous flow over nanohollow and nanostalagmite of taro leaf surface

5. 1. Tilt variation on the resulting voltage in the electric energy harvesting model.

Fig. 3 shows a graph of the voltage (Volt) with time (second) generated by water droplets when it comes in contact with the surface of taro leaves at various tilt angles, namely 0°, 15°, 30°, and 45°. This test was carried out by dropping water droplets on the leaves at a rate of 1 drop/s continuously for 500 seconds. At the start time, the graph shows the increase in voltage and over time the voltage starts to be constant. The greater the slope level, the greater the resulting voltage. It is marked with a black line for the slope of 0° at the bottom, red for a slope of 15°, blue for a slope of 30°, and purple for a slope of 45°. This happens because in the second stage of testing, the presence of a bridge rectifier and capacitor greatly affects the appearance of the graph. Bridge rectifier functions as a rectifier for AC to DC currents. AC current is generated by fluctuating electron jumps when water droplets come in contact with taro leaves and aluminum as electrodes.

The answer: In previous studies it is reported about the signal recorded without a bridge rectifier [26]. The research was conducted by looking at the signal in one water *drop*let for a slope of 0°, 15°, 30° and 45°. The voltage results are smaller than our present study. There are many voltage peaks that appear because the output is alternating current. Let's compare the 1 highest peak for each leaf slope. For this reason, let's conduct this research in order to see the behavior of further voltage.

When this test is varied as in the graphs in Fig. 4, 5, there is an increase in the value of the voltage (volt) compared to the graph in Fig. 3. In Fig. 4, shows the droplet rate (2 drop/s) contact with taro leaves for every second during 500 seconds. Meanwhile, Fig. 5 shows the droplet rate (3 drop/s) in contact with taro leaves for every second during 500 seconds. This clearly proves the phenomenon that the more water droplets in contact with the taro leaves, the more chance the atoms in the water droplets come into contact with the leaf surface. As such, more electrons are excited from their orbit, resulting in higher electrical energy in the form of voltage (volt).

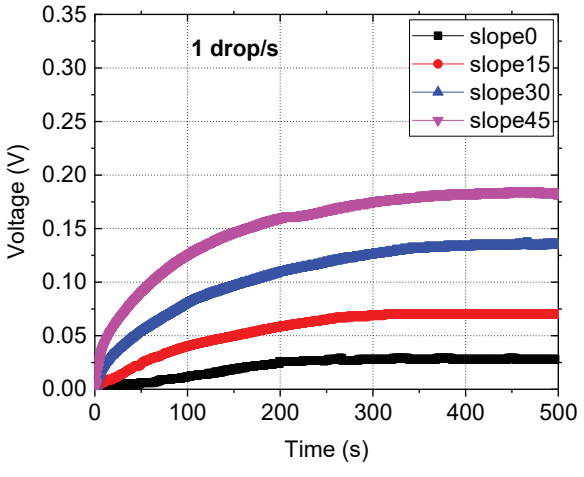

Fig. 3. Output voltage (V) generated by water droplets over taro leaves at a rate of 1 drop/s and a slope of 0°, 15°, 30°, 45° for 500 seconds

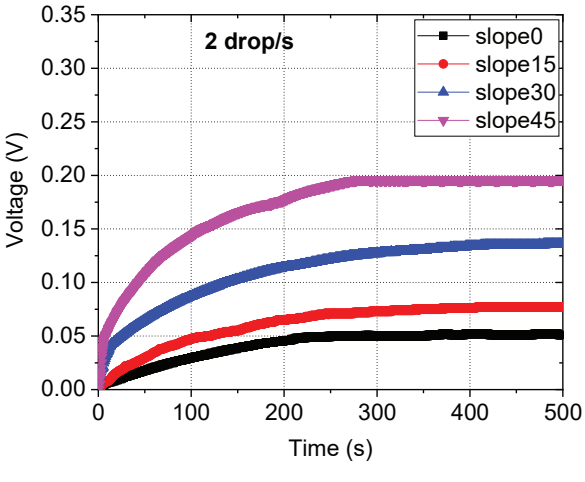

Fig. 4. Output voltage (V) generated by water droplets over taro leaves at a rate of 2 drop/s and a slope of 0°, 15°, 30°, 45° for 500 seconds

Taro leaves play an important role as a membrane in delivering ions to flow. With the bridge rectifier, this AC current is rectified into DC direct current. Then this current goes to the capacitor and is read as voltage (volt) on a digital multimeter. At the beginning of data collection,

there was an increase because the capacitor charging process was in progress. As the capacitor capacity began to full, the graph began to flatten and finally remained constant, with no significant increase or decrease. The voltage continues because water droplets are continuously dropped. In fact, it cannot be denied that if this event continues, the voltage will continue to be read even after the 500 seconds are over. However, because the graphical phenomenon shows a steady situation, the test is limited to 500 seconds.

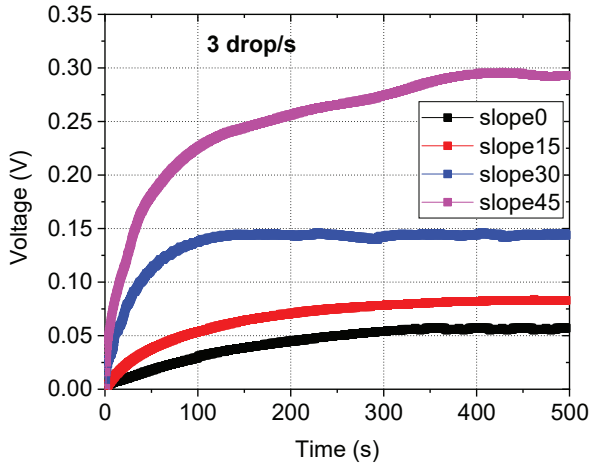

Fig. 5. Output voltage (V) generated by water droplets over taro leaves at a rate of 3 drop/s and a slope of 0°, 15°, 30°, 45° for 500 seconds

5. 2. SEM test results for nanostalagmite and nanohollow structure on the surface of taro leaves

To enlarge the surface of taro leaves, a Scanning electron microscope (SEM) is used. This is intended to observe the surface morphology of taro in more detail. The SEM composition test was carried out on the surface of the taro leaves with a waxy coating, the leaves were still green, fresh, not wilted, in good condition, and not damaged by human touch.

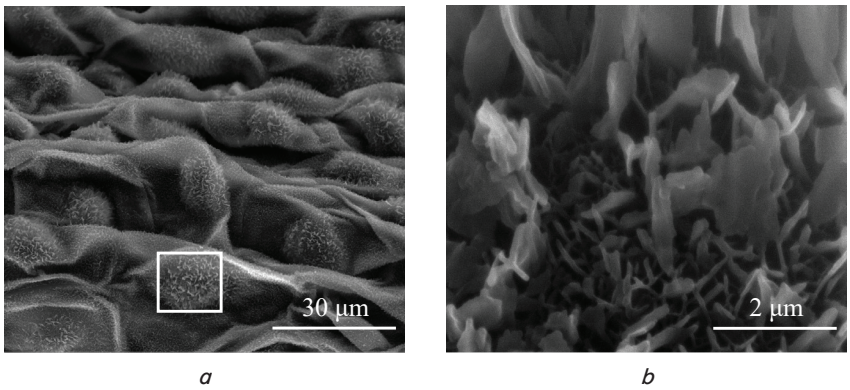

a *b*

Fig. 6. SEM test on the surface of taro leaves with waxy coating; *a* – SEM test 30 μm scale; *b* – SEM test 2 μm scale on the magnification of white box in Fig. 6, *a*

Fig. 6, *a* shows the result of SEM test for taro leaves with a 3000x magnification on a 30 μm scale. Then the white box shown in Fig. 6, *a* is magnified at 40,000x magnification at 2 *μm* scale as shown in Fig. 6, *b*. In Fig. 6, *a*, its morphological appearance resembles a sphere with hairs separated from other spheres, with a certain distance, scattered all over the surface. When the sphere is enlarged, the hairs appear more clearly to have a hedge of height, appear sharp and flat, protruding upwards.

6. Discussion from development of energy harvesting with water droplet continuous flow over nanohollow and nanostalagmite of taro leaf surface

In previous research it is reported about the use of natural materials as a superhydropobic surface. However only observed it for one water droplet. So that this research presents a method of harvesting electrical energy with a longer observation time. In this study only single droplets are used so that the current signal is not readable in the multimeter. It so small that more sensitive equipment is needed to detect the current signal.

The addition of capacitors and bridge rectifiers in the installation and water droplets are flowed continuously to see the behavior of the voltage that occurs during (dV/dT). The result is that there is a voltage that is measured, this is good in the process of harvesting electrical energy. In this research there are limitations, when the data collection process, the wax layer on the surface of the taro leaves is in a good condition. Not much damaged by human touch. A damaged wax layer will result in a reduced superhydropobic surface, the impact is that water droplets cannot fall and roll properly. This is important because it will greatly affect the voltage output on a digital multimeter. Sometimes these are so difficult to control that a closer look is needed. An electric current consists of a stream of tiny negatively charged particles called electrons. The excess or lack of electrons in the atom results in a charge imbalance in the atom. This charge imbalance is the beginning of the voltage difference. The jumping of electrons creates an electric voltage. The driving forces of this mechanism are surface tension and impulse force. The mechanism of electron jumping when a functional group contacts water droplets H^+ and OH^- is described in Fig. 7, 8.

Like the Grotthuss mechanism, in one water droplet there are H_2O molecules as shown in Fig. 7. Each water molecule is composed of two hydrogen atoms (H) which are covalently bonded to one oxygen atom (O) marked with a blue line. However, there are times when one H atom is hydrogen bonded (yellow line). When the H atom will hydrogen bond with the surrounding O atom, the H atom will be ionized from the previous O atom to become the H^+ ion (marked with the black dotted line). When these H^+ ions separate, what remains is the OH^- ion before finding a new H^+ (marked with a black dotted line). The OH^- ion will look for nearby H^+ ions to form new H_2O (indicated by the green dotted line). Conversely, the ionized H^+ will be drawn by the nearby OH^- ion to form new H_2O (marked with green dotted line). Finally, new H_2O molecules will form hydrogen bonds. And so on, this phenomenon repeats itself very quickly in one water droplet.

On the surface of the taro leaves, which have a waxy coating, there are several functional groups that resemble nanos-

talagmite [26]. One of them is the C-H (aromatic) functional group. Fig. 8 shows an illustration when water droplets come in contact with the R-(C_6H_5) (aromatic) functional groups on the surface of taro leaves. The R-(C_6H_5) functional group has the element H which is on the outer side of the taro leaf nanostalagmite. On the other hand, in one water droplet there are H_2O molecules. When the water droplet hits the R-(C_6H_5) (aromatic) functional group on the nanostalagmite of the surface of taro leaves, one H_2O molecule in one water droplet will ionize to become H^+ and OH^- ions. Then there is a release of one electron when OH^- attracts element H which tends to be positive on R-(C_6H_5) (green arrow). The H element is attracted to trigger out (marked with a red line going upwards), but when it is released, it meets H from H_2O which tends to be positive and ionizes to become H^+ and OH^- (red sign downward) to become H_2. When H of the functional group is pulled out, this position will be empty. Because C tends to be positive, OH^- will enter into binding to the functional group replacing the previous H position. As such, the end result of this interaction is the release of hydrogen (H_2) and one electron flows from H_2O (liquid) through nanostalagmite (solid) to the electrode.

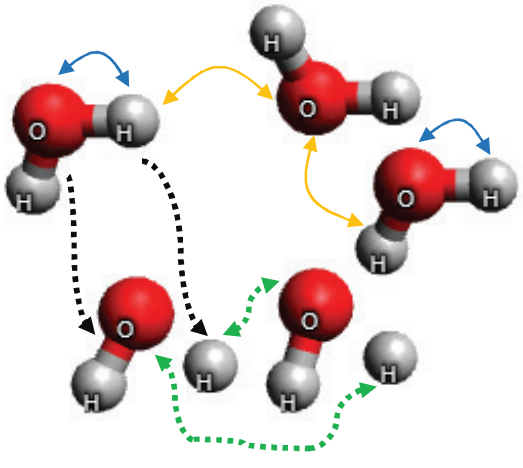

Fig. 7. An illustration of H_2O molecule in a water droplet

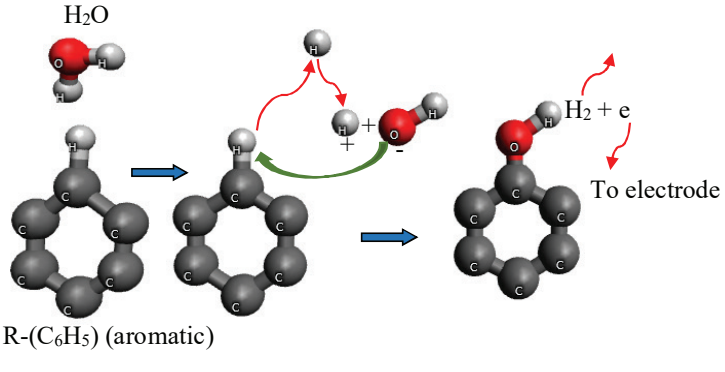

Fig. 8. An illustration of H_2O molecule becoming ionized into OH^- and OH^+ when water droplet comes in contact with R-(C_6H_5) (aromatic) functional group on the taro leaf surface

When leaves that have morphology such as nanostalagmites come into contact with H_2O droplets, the surface energy is very high. This affects the water molecules on the surface that have very strong bonds between molecules. In H_2O molecules there are two bonds, namely a covalent bond and a weaker hydrogen bond. These bonds are what support the surface tension in the droplets when in contact with the taro leaves.

The surface tension that occurs in the droplet is equivalent to the surface energy divided by the area of the contact area between the droplet and the surface ($\gamma \approx E/A$). When the cross-sectional area is very small (on the nanostalagmites), the energy becomes infinite. This large energy is transferred to the nanoparticles on the surface of the stalagmite so that these particles will vibrate violently and break through the droplet surface tension causing random motion. The random motion of particles in a fluid caused by collisions of solid particles with fluid molecules. When the particles get smaller, the random motion increases its energy and velocity. So, at the time of the water droplets hit the surface of the nanostalagmite for the first time, the H_2O molecules will break down into the equation below:

$$H_2O = H^+ + OH^-. \quad (1)$$

Furthermore when OH^- attracts element H which tends to be positive on C-H nanostalagmite (green arrow). The H element is attracted to trigger out (marked with a red line going upwards) there is a release electron. When H of the functional group is pulled out, this position will be empty. Because C tends to be positive, OH^- will enter into binding to the functional group replacing the previous H position. As such, the end result of this interaction is the release of one electrons flows from H_2O (liquid) through nanostalagmite (solid) to the electrode.

SEM result in Fig. 6, *b* was processed using ImageJ software to produce images such as the illustration in Fig. 9, *a*. Between one nanostalagmite and the other nanostalagmite was separated by a nanoscale hollow. There are countless nanoscale hollows. The more height and presence of nanostalagmites, the more areas of the nanoscale hollow. Fig. 8, 9, *a* show a very close relationship, as shown in Fig. 9, *b*. Initially, of the FTIR results [26] appeared peak 765,74; 815,89; 885,33. Referring to [27] table a simplified correlation chart, page 26 frequency peak between 900–690 cm^{-1} is C-H aromatic (out of plane bend). Writing C-H (aromatic) in Fig. 9, *b* follows the writing in the book [27]. In previous research, this protrusion was termed nanostalagmite which consists of chains of functional groups [26].

Fig. 9, *b* shows that the area marked with F_1 is the nanostalagmite region. Nanostalagmite has a chain of functional groups, one of which is the R-(C6H5) (aromatic) functional groups attached to the entire surface of F_1. A large number of nanoscale hollows exist between the F_1 region denoted by the F_2 region. The surface morphology of taro leaves such as the F_1 area makes water droplets marked with the F_3 area unable to enter the F_2 area. The ionized H_2O becomes H^+ and OH^- in contact with one R-(C_6H_5) (aromatic) functional group in the F_1 area. The yellow circle in Fig. 9, *b* is the location for hydrogen (H_2) production and electron excitation occurs as previously described in Fig. 8. As a result, if there is continuous contact between F_1 and F_3 then a lot of Hydrogen (H_2) is trapped in the F_2 area. If the particles in the F_1 area get smaller, the energy will be even greater, causes Hydrogen (H_2) to try to get out to push the water droplets in the form of a liquid. The wider the F_2 area, the more electron flows from H_2O (liquid) through nanostalagmite (solid) to the electrode.

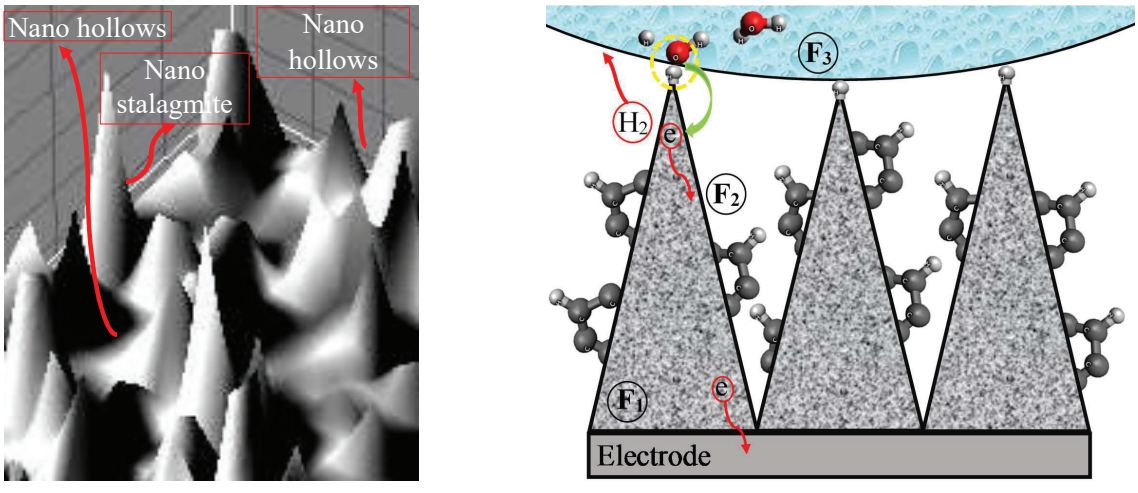

a *b*

Fig. 9. An illustration of taro leaf surface contact with water droplets; *a* – Location of nanoscale hollows between nanostalagmites; *b* – Location of group R-(C_6H_5) (aromatic) functional group in F_1 producing H_2 where the release of electron

Electron excitation will also continue to increase along with the higher the rate of water droplets in contact with the leaf surface continuously for 500 seconds. When the field is getting tilted the water droplet will be affected by the force of gravity, the weight of the water particles will press the particles below, then the water particles below will press each other to the bottom of the water so that the pressure below will be greater than the upper pressure. Atoms such as H^+ and OH^- which ionize from the H_2O molecules will center to the bottom of the droplet as well. As a result, more H^+ and OH^- atoms interact with functional groups in the F_1 region. This is the cause of the measured voltage (Volt) getting higher as shown in the graphs in Fig. 3–5. The voltage output was consistence because there are so many droplets that fall over the leaf continuously for 500 seconds.

Water droplets actually come into contact with the air on the leaf surface. Therefore, it can be considered that the interface of compounds is heterogeneous surface, and the relationship between surface wettability and surface roughness can be well explained by the Cassie and Baxter equations [28]. If the water droplet has zero hydrostatic pressure, the water droplet will stop on the surface of the nanostalagmite.

For example, F_{13} becomes the total area of the solid-liquid interface and F_{23} becomes the total area of the liquid-air interface (air in the hollow area) in the plane parallel to the rough surface of the taro leaves. When the water disperses, the solid-air interface in area F_{13} is destroyed and an energy of $F_{13}\gamma_{SA}$ is obtained, where γ_{SA} is the energy of the solid-air interface. Energy $F_{13}\gamma_{LS}$ is released to form a solid-liquid interface in the same area, where γ_{LS} is the energy of the solid-liquid interface. Energy $F_{23}\gamma_{LA}$ is also released to form a water-air surface. Therefore, the net energy, E_D, which is expended in the formation of the interface geometric units is:

$$E_D=F_{13}(\gamma_{LS}-\gamma_{SA})+F_{23}\gamma_{LA}. \quad (2)$$

If θ_A is the contact angle of the solid-liquid interface,

$$\cos\theta_A=(\gamma_{SA}-\gamma_{LS})/\gamma_{LA}. \quad (3)$$

Equation 2 becomes:

$$E_D=\gamma_{LA}(F_{23}-F_{13}\cos\theta_A). \quad (4)$$

Equation 3 can be written as:

$$\cos\theta_A=-E/\gamma_{LA}. \quad (5)$$

Since $(\gamma_{LS}-\gamma_{SA})$ is energy (E) required to form an area unit of the solid-liquid interface, a contact angle (θ_D) can be determined for the porous surface of the nanostalagmite with the (5) analogy:

$$\cos\theta_D=-E_D/\gamma_{LA}=F_{13}\cos\theta_A-F_{23}. \quad (6)$$

When the surface is rough but nonporous, F_{23} is zero. The equation (6) is for the contact angle of the rough surface with the roughness factor of F_{13}. Equation (6) shows the contact angle for water moving forward on a dry surface. Contact angles visible can be defined using the same principle:

$$\cos\theta_W=F_{13}\cos\theta_R-F_{23}. \quad (7)$$

Where θ_R is the contact angle between the solid and the liquid, and θ_W is the contact angle on the porous surface. It should be noted that F_{13} and F_{23} in the equation (7) are determined by the contact angle θ_A. From the elaboration of equation (7), for a surface consisting of 2 fractions, the first fraction has a F_{13} fractional area and a θ_{13} contact angle. The second fraction has a F_{23} fractional area and a θ_{23} contact angle. Then, the equation becomes:

$$\cos\theta=F_{13}\cos\theta_1+F_{23}\cos\theta_{23}. \quad (8)$$

From equation (8) it can be simplified to $F_1+F_2=1$, where F_1 and F_2 are the fractional areas estimated for solids and air trapped between the surface of the nanostalagmite and the water droplet, respectively. This equation shows that the larger the air fraction (F_2), the more hydrophobic the surface will be. Namely, most of the air, in this case the hydrogen (H_2) trapped in the surface gap, greatly increases the contact between air and water, effectively preventing

water droplet penetration into the nanohollow. This is what makes the surface of taro leaves has superhydropobic characteristics/is not wetted by water. The weakness of this study is the limited quantity of leaves available when collecting the data. To prevent this happening, it is necessary to cultivate taro leaves so that they can be used to generate electrical energy in the future for a longer period of time. Experimentally this research focuses on taro leaf material only, so that further research is needed with other hydrophobic leaf materials to reveal the performance of electrical energy generated when in contact with water droplets. For example, such as lotus leaves that have superhydropobic properties. It can be observed morphology, functional groups and chemical elements. In addition, to use water droplets using direct rainwater, differences in voltage behavior were observed compared to using pure water. In the future, as an alternative to hydrophobic materials that can be used as an environmentally friendly produce of electrical energy.

7. Conclusions

1. Taro leaves (Colocasia esculenta L) from natural materials are an effective ingredient for generating electrical energy. This mechanism occurs when the surface of the leaf is coated as aluminum foil under it as an electrode in contact with water droplets that are flowed continuously. Taro leaves play an important role as a membrane in delivering ions to flow. With the bridge rectifier, this AC current is rectified into DC direct current. The highest stress at a slope of 45° was generated at a water droplet rate of 1 drop/s, 2 drop/s, 3 drop/s, is 0.185 V; 0.196 V; 0.295 V respectively. This clearly proves the phenomenon that the more the water droplets and the greater the inclination of the plane, the more likely the atoms in the water droplet will come into contact with the leaf surface. Thus, more electrons are excited from their orbits, resulting in a higher electrical energy in the form of a voltage.

2. The SEM results show that taro leaves surface is made by a cluster of nanostalagmites with other nanostalagmites separated by nanoscale hollows that tend to repel water droplets. The consequence of the repulsion of nanoscale stalagmites at a very small radius of the stalagmite nanostructure are very high surface tension or surface energy. One of the factors for electron jump is generated due to the high surface tension energy of the nanostalagmite structure when in contact with H^+ and OH^- ionized in water droplets to produce hydrogen (H_2).

The excited electrons from the H_2O in the water droplet when hitting the nanostalagmites will cause an electron jump. The electron flows from H_2O (liquid) through nanostalagmite (solid) interphase surface to the electrode.

Acknowledgments

The author would like to thank the financial support from the Directorate General of Higher Education, Ministry of Research, Technology and Higher Education of the Republic of Indonesia which was provided through the PDD scheme with contract number 1/E/KPT/2018. Thanks also to Ngafwan and I. G. K Puja for their contribution to the discussion of the functional groups of nanostalagmites with their electron mobility, which have supported this research work.

Reference

1. Webb, H. K., Crawford, R. J., Ivanova, E. P. (2014). Wettability of natural superhydrophobic surfaces. Advances in Colloid and Interface Science, 210, 58–64. doi: https://doi.org/10.1016/j.cis.2014.01.020
2. Negara, K. M. T., Wardana, I. N. G., Widhiyanuriyawan, D., Hamidi, N. (2019). The Role of the Slope on Taro Leaf Surface to Produce Electrical Energy. IOP Conference Series: Materials Science and Engineering, 494, 012084. doi: https://doi.org/10.1088/1757-899x/494/1/012084
3. Lee, Y. R., Shin, J. H., Park, I. S., Rhee, K., Chung, S. K. (2015). Energy harvesting based on acoustically oscillating liquid droplets. Sensors and Actuators A: Physical, 231, 8–14. doi: https://doi.org/10.1016/j.sna.2015.03.009
4. Lin, Z.-H., Cheng, G., Lee, S., Pradel, K. C., Wang, Z. L. (2014). Harvesting Water Drop Energy by a Sequential Contact-Electrification and Electrostatic-Induction Process. Advanced Materials, 26 (27), 4690–4696. doi: https://doi.org/10.1002/adma.201400373
5. Baytekin, B., Baytekin, H. T., Grzybowski, B. A. (2012). What Really Drives Chemical Reactions on Contact Charged Surfaces? Journal of the American Chemical Society, 134 (17), 7223–7226. doi: https://doi.org/10.1021/ja300925h
6. Wu, W., Wang, X., Liu, X., Zhou, F. (2009). Spray-Coated Fluorine-Free Superhydrophobic Coatings with Easy Repairability and Applicability. ACS Applied Materials & Interfaces, 1 (8), 1656–1661. doi: https://doi.org/10.1021/am900136k
7. Luo, Z. Z., Zhang, Z. Z., Hu, L. T., Liu, W. M., Guo, Z. G., Zhang, H. J., Wang, W. J. (2008). Stable Bionic Superhydrophobic Coating Surface Fabricated by a Conventional Curing Process. Advanced Materials, 20 (5), 970–974. doi: https://doi.org/10.1002/adma.200701229
8. Ma, X., Zhao, D., Xue, M., Wang, H., Cao, T. (2010). Selective Discharge of Electrostatic Charges on Electrets Using a Patterned Hydrogel Stamp. Angewandte Chemie, 122 (32), 5669–5672. doi: https://doi.org/10.1002/ange.201000766
9. Zhao, D., Duan, L., Xue, M., Ni, W., Cao, T. (2009). Patterning of Electrostatic Charge on Electrets Using Hot Microcontact Printing. Angewandte Chemie International Edition, 48 (36), 6699–6703. doi: https://doi.org/10.1002/anie.200902627
10. Lin, Z.-H., Zhu, G., Zhou, Y. S., Yang, Y., Bai, P., Chen, J., Wang, Z. L. (2013). A Self-Powered Triboelectric Nanosensor for Mercury Ion Detection. Angewandte Chemie International Edition, 52 (19), 5065–5069. doi: https://doi.org/10.1002/anie.201300437

11. Fan, F.-R., Tian, Z.-Q., Lin Wang, Z. (2012). Flexible triboelectric generator. Nano Energy, 1 (2), 328–334. doi: https://doi.org/10.1016/j.nanoen.2012.01.004
12. Cheng, G., Lin, Z.-H., Lin, L., Du, Z., Wang, Z. L. (2013). Pulsed Nanogenerator with Huge Instantaneous Output Power Density. ACS Nano, 7 (8), 7383–7391. doi: https://doi.org/10.1021/nn403151t
13. Zhu, G., Lin, Z.-H., Jing, Q., Bai, P., Pan, C., Yang, Y. et. al. (2013). Toward Large-Scale Energy Harvesting by a Nanoparticle-Enhanced Triboelectric Nanogenerator. Nano Letters, 13 (2), 847–853. doi: https://doi.org/10.1021/nl4001053
14. Nguyen, V., Yang, R. (2013). Effect of humidity and pressure on the triboelectric nanogenerator. Nano Energy, 2 (5), 604–608. doi: https://doi.org/10.1016/j.nanoen.2013.07.012
15. Zhang, X.-S., Han, M.-D., Wang, R.-X., Zhu, F.-Y., Li, Z.-H., Wang, W., Zhang, H.-X. (2013). Frequency-Multiplication High-Output Triboelectric Nanogenerator for Sustainably Powering Biomedical Microsystems. Nano Letters, 13 (3), 1168–1172. doi: https://doi.org/10.1021/nl3045684
16. Roundy, S., Wright, P. K. (2004). A piezoelectric vibration based generator for wireless electronics. Smart Materials and Structures, 13 (5), 1131–1142. doi: https://doi.org/10.1088/0964-1726/13/5/018
17. Guigon, R., Chaillout, J.-J., Jager, T., Despesse, G. (2008). Harvesting raindrop energy: experimental study. Smart Materials and Structures, 17 (1), 015039. doi: https://doi.org/10.1088/0964-1726/17/01/015039
18. Al Ahmad, M., Jabbour, G. E. (2012). Electronically droplet energy harvesting using piezoelectric cantilevers. Electronics Letters, 48 (11), 647. doi: https://doi.org/10.1049/el.2012.0616
19. Feng, L., Liu, Y., Zhang, H., Wang, Y., Qiang, X. (2012). Superhydrophobic alumina surface with high adhesive force and long-term stability. Colloids and Surfaces A: Physicochemical and Engineering Aspects, 410, 66–71. doi: https://doi.org/10.1016/j.colsurfa.2012.06.018
20. Zhang, X., Guo, Y., Zhang, P., Wu, Z., Zhang, Z. (2012). Superhydrophobic and Superoleophilic Nanoparticle Film: Synthesis and Reversible Wettability Switching Behavior. ACS Applied Materials & Interfaces, 4 (3), 1742–1746. doi: https://doi.org/10.1021/am201856j
21. Yuan, Y., Lee, T. R. (2013). Contact Angle and Wetting Properties. Springer Series in Surface Sciences, 3–34. doi: https://doi.org/10.1007/978-3-642-34243-1_1
22. Feng, L., Zhang, H., Mao, P., Wang, Y., Ge, Y. (2011). Superhydrophobic alumina surface based on stearic acid modification. Applied Surface Science, 257 (9), 3959–3963. doi: https://doi.org/10.1016/j.apsusc.2010.11.143
23. Seo, H. O., Kim, K.-D., Jeong, M.-G., Kim, Y. D., Choi, K. H., Hong, E. M. et. al. (2011). Superhydrophobic carbon fiber surfaces prepared by growth of carbon nanostructures and polydimethylsiloxane coating. Macromolecular Research, 20 (2), 216–219. doi: https://doi.org/10.1007/s13233-012-0029-y
24. Subagyo, R., Wardana, I. N. G., Widodo, A., Siswanto, E. (2017). The Mechanism of Hydrogen Bubble Formation Caused by the Super Hydrophobic Characteristic of Taro Leaves. International Review of Mechanical Engineering (IREME), 11 (2), 95. doi: https://doi.org/10.15866/ireme.v11i2.10621
25. Negara, K. M. T., Widhiyanuriyawan, D., Hamidi, N., Wardana, I. N. G. (2020). The Dynamic Interaction of Water Droplet with Nano-Stalagmite Functional Groups of Taro Leaf Surface. Journal of Southwest Jiaotong University, 55 (2). doi: https://doi.org/10.35741/issn.0258-2724.55.2.28
26. Kriz, G. S., Pavia, D. L., Lampman, G. M. (2001). Introduction to Spectroscopy. Washington.
27. Cassie, A. B. D., Baxter, S. (1944). Wettability of porous surfaces. Transactions of the Faraday Society, 40, 546. doi: https://doi.org/10.1039/tf9444000546